Journal of Information Systems Engineering and Management
2025, 10(62s)
e-ISSN: 2468-4376
https://jisem-journal.com/

Research Article

Effect of Chirality on Transmission in an Optical Fiber

Mohamed Lotfi Cherrad[1], Toufik Achour[1], Mohamed Chaour[1], Sofiane Boulkroune[1], Billel Hamadi[1], Djamel Boucherma[1], Khaled Chettah[1]
[1]*Research Center in Industrial Technologies CRTI, P.O. Box 64, Cheraga, 16014 Algiers, Algeria*

ARTICLE INFO

Received: 30 May 2025
Revised: 15 Sept 2025
Accepted: 02 Nov 2025

ABSTRACT

This study examines how bianisotropic chirality, introduced through $LiNbO_3$ material in the core, affects mode propagation in an asymmetric optical fiber. Numerical solutions of the dispersion equations using the Newton-Raphson method enabled accurate evaluation of propagation behavior. The findings show that increasing the chirality parameter enhances the propagation constants and slightly reduces cutoff frequencies. As a result, the fundamental mode carries more transmitted power, improving field confinement. Chirality also reduces attenuation, allowing longer transmission distances. Overall, the results indicate that incorporating chirality can optimize fiber performance for telecommunications and sensing.

Keywords: chirality, optical fiber, bianisotropic, Magnetic Field, Electric Field

1. INTRODUCTION

Chirality, or optical activity, has attracted extensive theoretical and experimental attention [1,7]. In the field of optics, this phenomenon has various applications, including mode conversion [1,8], Fiber switching [5], and optical Fiber transmission [7]. Chirality, or optical activity, has attracted extensive theoretical and experimental attention [1,7]. In the field of optics, this phenomenon has various applications, including mode conversion [1,8], Fiber switching [5], and optical Fiber transmission [7].

In this study, we explore the effects of Bianisotropic chirality in $LiNbO_3$ materials on the propagation modes within asymmetrical optical Fibers, aiming to bridge gaps in theoretical knowledge regarding chiral interactions in optical systems. Practically, our findings support enhanced Fiber design for telecommunications by optimizing mode propagation characteristics, thus enabling higher transmission efficiency and potential applications in advanced sensing technologies. The objective of this article is to investigate the impact of anisotropic chirality in $LiNbO_3$ core materials on the propagation constants, cutoff frequencies, and overall mode behavior in asymmetrical optical Fibers. By analyzing how variations in chirality affect signal transmission and Fiber performance, we aim to identify optimal conditions for maximizing data transmission rates and power handling capabilities, ultimately contributing to advanced Fiber designs in telecommunications and sensing technologies.

2. ELECTROMAGNETIC ANALYSIS OF CHIRAL OPTICAL FIBERS

The modeled optical fiber structure is as follows:

• Core (silica doped with $LiNbO_3$): The core composition is modified by introducing a small amount of $LiNbO_3$, inducing anisotropy and chirality.

• Cladding (pure silica): The cladding remains pure silica to preserve a high refractive index contrast, as illustrated in Figure 1.

Journal of Information Systems Engineering and Management
2025, 10(62s)
e-ISSN: 2468-4376
https://jisem-journal.com/

Research Article

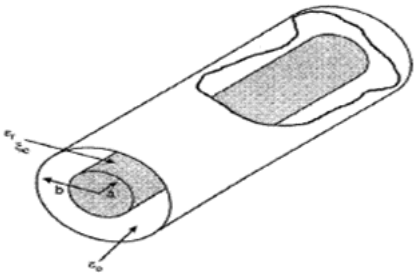

Figure 1. Fiber optic chiral core.

Using the following constitutive relatives [4]:

$$D = \varepsilon_0 \varepsilon E + j\sqrt{\mu_0 \varepsilon_0}\,\xi H$$
$$B = \mu_0 \mu H - j\sqrt{\mu_0 \varepsilon_0}\,\xi E \qquad \text{(Eq. 1)}$$

And considering the dual anisotropy material parameters:

$$\varepsilon = \begin{bmatrix} \varepsilon_r & 0 & 0 \\ 0 & \varepsilon_\theta & 0 \\ 0 & 0 & \varepsilon_z \end{bmatrix}, \quad \mu = \begin{bmatrix} \mu_r & 0 & 0 \\ 0 & \mu_\theta & 0 \\ 0 & 0 & \mu_z \end{bmatrix}, \quad \xi = \begin{bmatrix} \xi_r & 0 & 0 \\ 0 & \xi_\theta & 0 \\ 0 & 0 & \xi_z \end{bmatrix} \qquad \text{(Eq. 2)}$$

Where: are the chirality tensor, permeability and permittivity. After developing the analytical equations of Maxwell, we derived the transverse components of the electric and magnetic fields from the longitudinal components required for establishing the differential equations, which were subsequently verified using the longitudinal components.

2.1 Calculation of transverse components of electric and magnetic fields based on longitudinal components

Algebraic manipulations, led us to the two following differential equations for the electric field:

$$\left(\frac{\partial^2 E_r}{\partial r^2} + \frac{1}{r}\frac{\partial E_r}{\partial r}\right) + \left[\left(\mu_0 \varepsilon_0 (\xi_z{}^2 + \mu_z \varepsilon_z)\omega^2 - \beta^2\right) - \frac{\upsilon^2}{r^2}\right] E_r = 1$$
$$\left(\frac{\partial^2 E_\theta}{\partial \theta^2}\right)\frac{1}{\psi_\theta} = -\upsilon^2 \qquad \text{(Eq. 3)}$$

And the magnetic field we have:

$$\left(\frac{\partial^2 H_r}{\partial r^2} + \frac{1}{r}\frac{\partial H_r}{\partial r}\right) + \left[\left(\mu_0 \varepsilon_0 (\xi_z{}^2 + \mu_z \varepsilon_z)\omega^2 - \beta^2\right) - \frac{\upsilon^2}{r^2}\right] H_r = 1$$
$$\left(\frac{\partial^2 H_\theta}{\partial \theta^2}\right)\frac{1}{\psi_\theta} = -\upsilon^2 \qquad \text{(Eq. 4)}$$

Equations (3-4) leading to the following wave equations:

$$\begin{pmatrix} E_{z1} \\ H_{z1} \end{pmatrix} = \begin{pmatrix} E_1 \\ H_1 \end{pmatrix} J_\upsilon\left(U\frac{r}{a}\right) e^{j\upsilon\theta} e^{-j\beta z} \qquad \text{(Eq. 5)}$$

Journal of Information Systems Engineering and Management
2025, 10(62s)
e-ISSN: 2468-4376
https://jisem-journal.com/

Research Article

E1, H1: Constant relative amplitudes of the fields E and H.

2.2 Dispersion equation

After expressing the longitudinal components at the core and the cladding while considering the boundary conditions imposed by the considered structure (Figure 1) we obtain the following equation:

$$(U\frac{J'_\upsilon(U)}{J_\upsilon(U)} - W\frac{J'_\upsilon(W)}{J_\upsilon(W)}) = 0 \quad \text{(Eq.6)}$$

Where the propagation constants in the core and the cladding are respectively:

$$U^2 = (\mu_0\varepsilon_0(\xi_z{}^2 + \mu_z\varepsilon_z)\omega^2 - \beta^2)a^2 \quad \text{(Eq.7)}$$

$$W^2 = k^2a^2 = a^2(\beta^2 - k_0^2n_2^2) \quad \text{(Eq.8)}$$

2.3 Cutoff frequencies

The cutoff frequencies are defined when the electromagnetic fields instead of propagating in the core, they are radiated completely in the cladding, and that is: W = 0. The normalized frequency is given by:

$$V_C = ak_0\sqrt{(\xi^2 + \mu\varepsilon - n_2^2)} \quad \text{(Eq. 9)}$$

2.4 Chirality's impact on performance

In this section, we introduce small amounts of chiral material into the core of optical fibers composed of weak magnetic dielectrics.

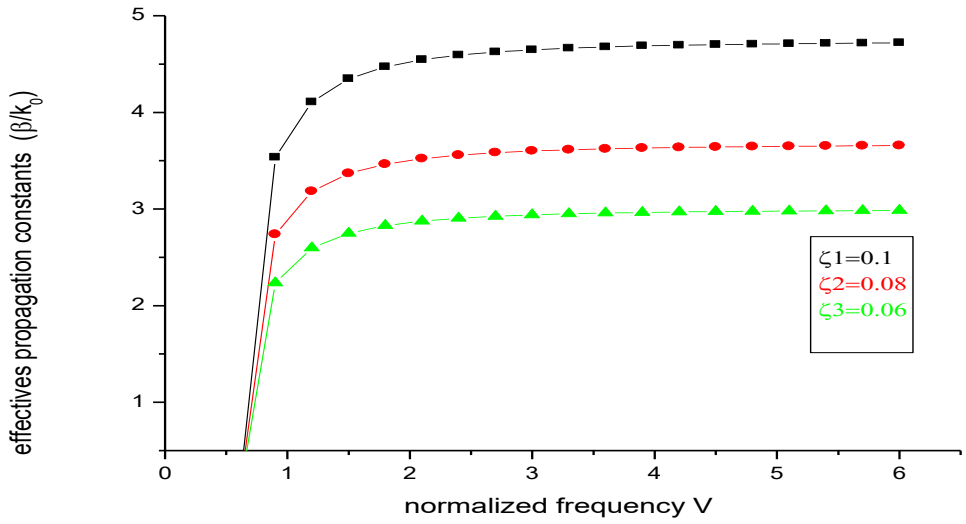

Figure 2. effectives propagation constants of HE11 modes depending of the frequency (2a=3.45µm, ε1=5.12, µ1= 1.48).

Journal of Information Systems Engineering and Management
2025, 10(62s)
e-ISSN: 2468-4376
https://jisem-journal.com/

Research Article

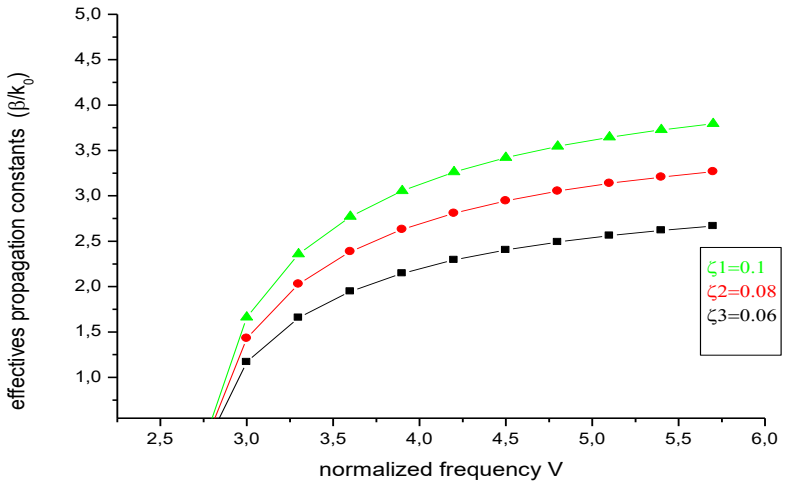

Figure 3. effectives propagation constants of HE12 modes depending of the frequency (2a=3.45µm, ε1=5.12, µ1= 1.48).

Figures 2 and 3 illustrate the effect of core chirality on the propagation modes in detail. We observe that an increase in core chirality results in higher propagation constants for the HE12 modes, along with a decrease in their cutoff frequencies. This behavior suggests that the chiral nature of the core enhances the coupling strength for the HE12 modes, enabling them to propagate more effectively at lower frequencies. Conversely, for the HE11 modes, while the propagation constants also increase with core chirality, there is no significant effect on their cutoff frequencies. This indicates that the HE11 modes are less sensitive to changes in chirality when compared to the HE12 modes, suggesting a potential decoupling between mode propagation characteristics and core structure for certain modes. These observations underscore the complex influence of chirality on wave propagation, potentially impacting the design and optimization of chiral waveguides for specific applications in optical communications.

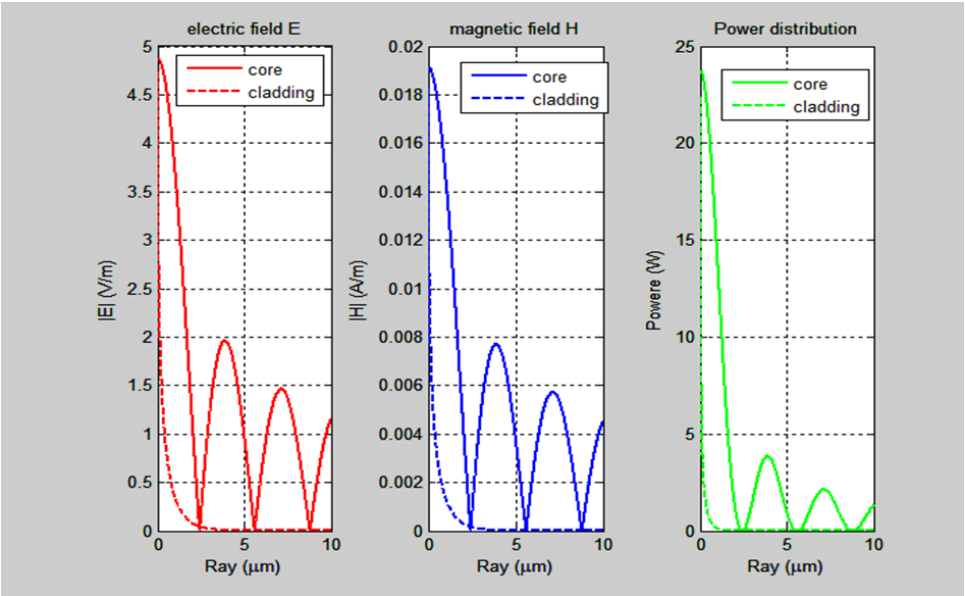

Figure 4. Electric and magnetic field distributions, along with optical power propagation in the Fiber.

Journal of Information Systems Engineering and Management
2025, 10(62s)
e-ISSN: 2468-4376
https://jisem-journal.com/

Research Article

Figure 4 illustrates the intensity distributions of the electric and magnetic fields, along with the optical power propagation within the core and cladding of the optical Fiber. In the first plot, the electric field distribution is shown. The field amplitude reaches its maximum at the center of the core and gradually decreases toward the edges. In the cladding (substrate), the intensity drops rapidly, indicating a slight leakage of the optical signal outside the core.

The second plot presents the magnetic field distribution. As expected, the magnetic field is coupled with the electric field and exhibits a similar spatial pattern. It is strongly confined within the core and significantly reduced in the cladding, confirming efficient light guidance.

The third plot displays the optical power distribution. The majority of the power is concentrated in the core, ensuring effective signal transmission. A small portion of the power, however, leaks into the cladding, resulting in minimal optical losses. This leakage is characterized by an exponential decay of the power intensity outside the core.

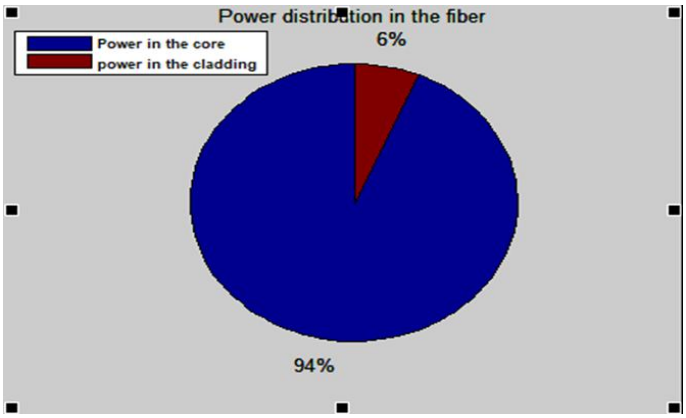

Figure 5. Power Confinement Percentage – Chiral Fiber.

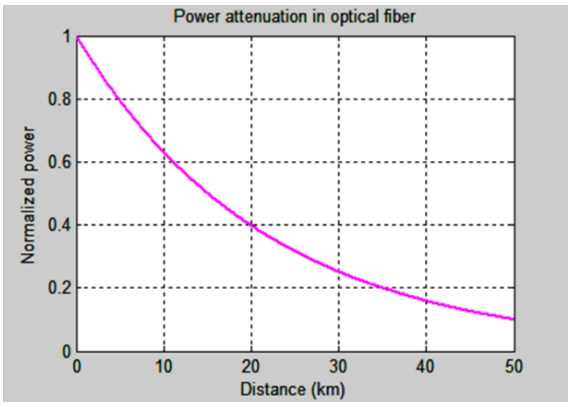

Figure 6. Optical Attenuation in Chiral Fibers.

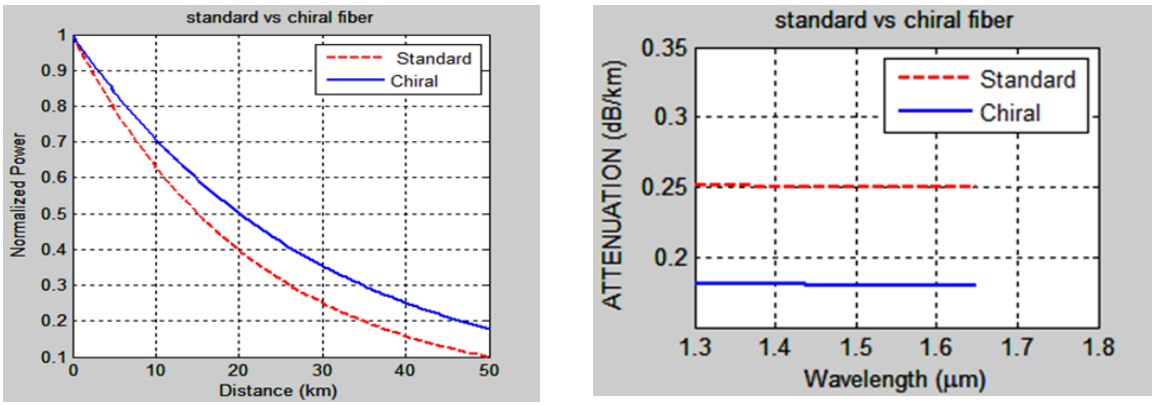

Figure 7. Optical Attenuation in Classic and Chiral Fibers: Comparison over Distance and Wavelength.

Figures 5 through 7 highlight the impact of chirality on the optical performance of Fibers, particularly in terms of power confinement and attenuation characteristics.

Figure 5 presents a pie chart that illustrates the optical power distribution between the core and cladding in a chiral-doped Fiber. The incorporation of chirality in the Fiber core leads to a significant increase in power confinement, with approximately 94% of the total optical power confined within the core. This enhanced confinement results from the modified effective refractive index profile introduced by the chiral doping, which improves the guiding efficiency and minimizes power leakage into the cladding.

Figure 6 compares the attenuation behavior as a function of propagation distance between a conventional (non-chiral) Fiber and a chiral-doped Fiber. The results clearly show that the chiral Fiber exhibits reduced attenuation, enabling the light to travel longer distances with less loss. This demonstrates the effectiveness of chirality in reducing propagation losses, thereby enhancing the transmission range.

Figure 7 shows the spectral attenuation curve α(λ) across a typical wavelength range used in optical communication. A notable minimum in attenuation is observed near 1.55 μm, which corresponds to the optimal transmission window in silica Fibers. The chiral Fiber's attenuation curve lies consistently below that of the conventional Fiber across the entire wavelength range, further confirming the improved transmission efficiency and broader bandwidth performance provided by the chiral modification.

Overall, these results demonstrate that chirality in the Fiber core not only improves power confinement but also significantly reduces attenuation, both with respect to distance and wavelength. This makes chiral-doped Fibers promising candidates for high-performance and long-distance optical communication systems.

3. CONCLUSION

This study explored the influence of bianisotropic chirality in $LiNbO_3$-doped cores on the performance of asymmetrical optical Fibers. The results clearly demonstrate that introducing chirality to the core material significantly improves optical confinement and reduces attenuation, enhancing the overall performance of the Fiber. By increasing the anisotropic chirality of the core, the effective refractive index is modified, leading to improved signal transmission efficiency. A substantial portion of the optical power is confined within the core, ensuring effective guidance with minimal leakage into the cladding. Moreover, chirality plays a crucial role in reducing propagation losses, allowing light to travel longer distances with less attenuation. The reduction in cutoff frequencies for higher-order modes facilitates the potential for exciting additional modes, which could enhance the fiber's overall capacity. However, this also necessitates careful management of modal dispersion to avoid any negative impact on signal integrity. The findings suggest that adjusting the core chirality can lead to substantial improvements in both the power transmission efficiency and the propagation distance of optical signals. These enhancements position chiral-doped optical Fibers as promising candidates for advanced communication systems and optical sensing applications. Future research could investigate the impact of external factors, such as temperature variations and mechanical stress, on the performance of chiral Fibers. Additionally, exploring alternative chiral materials and Fiber geometries may provide further avenues to optimize performance for a wide range of applications.

REFRENCES

[1] Athanasiadis, S. C., & Roupa, P. (2022): Detection of Buried Chiral Objects Using Electromagnetic Scattering in Two Dimensions. In 2022 12th International Conference on Dependable Systems, Services and Technologies (DESSERT) (pp. 1-8). IEEE.
[2] Dezaki, S. K., Askarpour, A. N., & Abdipour, A. (2021):Circular dichroism spectroscopy and chiral sensing in optical fibers. Optics Express. vol.29, No.15, pp. 23096-23112. DOI : 10.1364/OE.426239.
[3] Dirbeba, G., Li, J., Cao, Y., Liu, X., Zhao, R., Zhang, Y., & Kalwe, J. (2024): Orbital angular momentum modes in dielectrically chiral-core fibers. Journal of Physics D: Applied Physics. vol.57, No.34, pp. 345103. DOI :10.1088/1361-6463/ad4a7f.
[4] Enriquez, J. A., & Torres, P. (2023):Theoretical and computational study of the effects of the complex chirality parameter in chiral-coated planar waveguides. Journal of the Optical Society of America B. vol. 40, No. 4, pp. C86-C95. DOI:10.1364/JOSAB.481534.
[5] Gelmecha, D. J., & Singh, R. S. (2024): Modulation instability in nonlinear chiral fiber. Journal of Optical Communications. vol. 44, No. s1, pp. s567-s575. DOI:10.1515/joc-2020-0130.
[6] Gizatulin, A., Meshkov, I., Vinogradova, I., Bagmanov, V., Grakhova, E., & Sultanov, A. (2020): Generation of vortex optical beams based on chiral fiber-optic periodic structures. Sensors . vol. 20, No. 18, pp. 5345. DOI: 10.3390/s20185345.

Journal of Information Systems Engineering and Management
2025, 10(62s)
e-ISSN: 2468-4376
https://jisem-journal.com/

Research Article

[7] Lakhtakia, A., Varadan, V. K., Varadan, V. V., & Claus, A. C. (1990): Time-harmonic electromagnetic fields in chiral media . Applied Optics . vol. 29, No 7. s1, pp.892.
[8] Oksanen, M., Koivisto, P. K., & Lindell, I. V. (1990) : Dispersion curves and fields for a chiral slab waveguide. NASA STI/Recon Technical Report N. vol.92, pp. 22781. DOI:10.1049/ip-h-2.1991.0054.
[9] Roth, P., Russell, P. S. J., Frosz, M. H., Chen, Y., & Wong, G. K. (2022): Modulational instability and spectral broadening of vortex modes in chiral photonic crystal fibers. Journal of Lightwave Technology. vol. 41, No. 7, pp.2061-2069. DOI:10.1109/JLT.2022.3187197.